# HMG-CoA reductase inhibition delays DNA repair and promotes senescence after tumor irradiation

**Elena V. Efimova[1], Natalia Ricco[1], Edwardine Labay[2], Helena J. Mauceri[2], Amy C. Flor[1], Aishwarya Ramamurthy[1], Harold G. Sutton[2], Ralph R. Weichselbaum[2,3] and Stephen J. Kron[1,3]**

[1] Department of Molecular Genetics and Cell Biology, The University of Chicago, Chicago, IL

[2] Department of Radiation and Cellular Oncology, The University of Chicago, Chicago, IL

[3] Ludwig Center for Metastasis Research, The University of Chicago, Chicago, IL

**Running title:** Pitavastatin as pro-senescent radiosensitizer

**Keywords:** Statin, drug repurposing, radiosensitizer, senescence

1

**Corresponding author:**

Stephen J. Kron

Molecular Genetics and Cell Biology

929 East 57th Street

Chicago, IL, 60637

Pnone: 773-834-0250

Fax: 773-702-4394

skron@uchicago.edu

2

## ABSTRACT

Despite significant advances in combinations of radiotherapy and chemotherapy, altered fractionation schedules and image-guided radiotherapy, many cancer patients fail to benefit from radiation. A prevailing hypothesis is that targeting repair of DNA double strand breaks (DSBs) can enhance radiation effects in the tumor and overcome therapeutic resistance without incurring off-target toxicities. Unrepaired DSBs can block cancer cell proliferation, promote cancer cell death and induce cellular senescence. Given the slow progress to date translating novel DSB repair inhibitors as radiosensitizers, we have explored drug repurposing, a proven route to improving speed, costs and success rates of drug development. In a prior screen where we tracked resolution of ionizing radiation-induced foci (IRIF) as a proxy for DSB repair, we had identified pitavastatin (Livalo), an HMG-CoA reductase inhibitor commonly used for lipid lowering, as a candidate radiosensitizer. Here we report that pitavastatin and other lipophilic statins are potent inhibitors of DSB repair in breast and melanoma models both *in vitro* and *in vivo*. When combined with ionizing radiation, pitavastatin increased persistent DSBs, induced senescence and enhanced acute effects of radiation on radioresistant melanoma tumors. shRNA knockdown implicated HMG-CoA reductase, farnesyl diphosphate synthase, and protein farnesyl transferase in IRIF resolution, DSB repair and senescence. These data confirm on-target activity of statins, though via inhibition of protein prenylation rather than cholesterol biosynthesis. In light of prior studies demonstrating enhanced efficacy of radiotherapy in patients taking statins, this work argues for clinical evaluation of lipophilic statins as non-toxic radiosensitizers to enhance the benefits of image-guided radiotherapy.

3

**INTRODUCTION**

Cancer cells are rarely intrinsically radiosensitive, but advances in image-guided radiotherapy allow radiation to be focused on the tumor, providing a significant therapeutic advantage. Nonetheless, radiation is often insufficient on its own. Concomitant genotoxic chemotherapy is highly effective as a radiosensitizer, but chemoradiotherapy incurs dose-limiting and debilitating normal tissue toxicities while offering relatively small gains in the therapeutic ratio. This has provided an impetus to identify radiosensitizers that enhance radiation effects in the tumor with minimal impact outside the radiation field (1).

The beneficial effects of radiotherapy are considered to be mediated by formation of DNA double strand breaks (DSBs). DSBs are potentially lethal damage insofar as cell division can result in loss of chromosome arms. When cells suffer DSBs that exceed capacity for repair, they may die via apoptosis, necrosis or mitotic catastrophe. Surviving damaged cells may undergo therapy-induced senescence (TIS), a persistent cell cycle arrest characterized by enlarged cell size and activation of a gene expression program leading to secretion of inflammatory mediators (2-5). TIS has been documented in diverse human tumors after treatment with radiation and/or chemotherapy. While considerable disagreement remains whether TIS is a desirable or detrimental outcome of treatment (6-10), several studies indicate that senescent cells can suppress proliferation of surviving tumor cells and/or promote anti-tumor immune response (5,11,12).

Agents targeting DSB repair (reviewed in (13-15)) are considered promising therapeutics based on their potential to exploit intrinsic features of cancer cells but may

4

also be particularly well-suited to application as radiosensitizers. Although two poly-ADP-ribose polymerase (PARP) inhibitors have been approved and others are in late development, other promising DNA repair inhibitors have been abandoned due to low efficacy and/or high toxicity. Given practical constraints, an attractive source of new radiosensitizers might be agents that already have well-established safety profiles such as known drugs approved for other indications. Indeed, repurposing or repositioning has broad value for oncology (16,17) and approved drugs have proven to be a rich source of candidate radiosensitizers (e.g. (18-20)). Our strategy was to screen *in vitro* for persistence of ionizing radiation-induced foci (IRIF), the modified chromatin domains that mark DSBs (18). Among hits that were validated by assaying enhanced growth delay after irradiation (21) was the 3-hydroxy-3-methylglutaryl-CoA (HMG-CoA) reductase inhibitor pitavastatin (22) (NK-104; Livalo, Kowa Pharmaceuticals).

HMG-CoA reductase is the rate-limiting enzyme in the mevalonate pathway, regulating synthesis of cholesterol and its isoprenoid intermediates, geranylgeranyl pyrophosphate (GGPP) and farnesyl pyrophosphate (FPP) (23,24). Modification by GGPP and/or FPP is essential for function of small GTPases, lamins and other proteins with key roles in proliferation, survival, invasion, metastasis, inflammation and immune response (25-27). Thus, by attenuating mevalonate synthesis, statins not only decrease cholesterol biosynthesis but have pleiotropic effects impinging on multiple cancer pathways. In particular, diverse prenylated proteins including Ras, Rho, Rac, Ran, and Rap GTPases and lamins regulate DNA repair, apoptosis, senescence, and/or mitosis, suggesting that effects on multiple targets might mediate statin interactions with radiation.

5

Taking advantage of the high percentage of adults treated with HMG-CoA reductase inhibitors (statins) to treat dyslipidemia or lower cardiovascular risk, multiple studies have associated use with lower incidence and/or mortality for diverse cancers (e.g. (28)). Several studies have linked statin use to improved outcomes after radiotherapy for prostate (29,30), rectal (31) and breast (32) cancers, although others report conflicting results. In turn, multiple studies have demonstrated statins can protect against normal tissue damage after radiation or chemotherapy (33,34).

Given the lack of consensus on interactions between HMG-CoA reductase inhibitors and radiotherapy, we examined the effects of statins on radiation response. Pitavastatin delayed DSB repair and increased cell senescence after irradiation, leading to prolonged tumor growth delay. Confirming "on target" effects, blocking protein farnesylation by RNA interference recapitulated pitavastatin's effects. Taken together with prior work, our data support repurposing pitavastatin or other lipophilic statins as radiosensitizers, with particular applications to image-guided radiotherapy.

## MATERIALS AND METHODS

### Cell lines and cell culture

The MCF7$^{Tet-On}$ Advanced human mammary carcinoma cell line was obtained from Clontech in 2007 and was frozen in liquid nitrogen after 3 to 5 passages as a stock. We used the previously reported MCF7$^{GFP-IBD}$ (35) where MCF7$^{Tet-On}$ Advanced was modified to express GFP fused to the 53BP1-IRIF binding domain (IBD) under tetracycline-inducible control. MCF7$^{GFP-IBD}$ cells were maintained in DMEM medium containing 4.5 g/L glucose (Gibco), 1% penicillin/streptomycin (Gibco) supplemented with 10% Tet-approved FBS from (Clontech) and cultivated less than 10 passages prior to use. The cells were tested for mycoplasma and authenticated by short tandem repeat profile (IDEXX BioResearch) prior to and after performing experiments. All experiments were performed from 3 to 10 passages after thawing cells. Mouse melanoma cell line B16.SIY was maintained in complete RPMI medium (Gibco) containing 1% penicillin/streptomycin supplemented with 10% FBS. The B16.SIY cells were a kind gift from T. Gajewski and used without authentication.

### Chemical probes

Statin drugs were obtained from commercial sources as follows: pitavastatin calcium from Atomole, lovastatin, pravastatin sodium and atorvastatin calcium from Toronto Research Chemicals, simvastatin from Cayman Chemical and rosuvastatin calcium from Biotang. Mevalonate pathway metabolites R-mevalonic acid sodium salt and farnesyl pyrophosphate ammonium salt were from Sigma and geranyl pyrophosphate ammonium salt was from Axon MedChem. PARP1/2 inhibitor veliparib (ABT-888) was obtained from Chemie Tek.

7

**shRNA knockdowns**

Pairs of Sigma MISSION shRNAs targeting expression of HMG-CoA reductase (HMGCR), farnesyl diphosphate synthase (FDPS), geranylgeranyl diphosphate synthase 1 (GGPS1), farnesyl diphosphate transferase beta (FNTB) and non-targeting scrambled (Scr) negative control plasmids were obtained in pLKO.1-puro vectors and used according to manufacturer's instructions. Lentivirus-containing supernatant was produced by transfection of the 293T Lenti-X cell line (Clontech) and applied to MCF7$^{Tet-On}$ cells. Following selection in the presence of puromycin, pairs of stable MCF7$^{Tet-On}$ cell lines with silencing of HMGCR, FDPS, GGPS1 and FNTB protein expression were established. Cells from the third passage post-selection were frozen in liquid nitrogen as a stock. Most experiments were done on 4-6 passages of established cell lines. At least 2 shRNA constructs targeting different sequences of corresponding mRNA were evaluated for each gene. Silencing of targeted genes was validated by Western blot. shRNAs and antibodies used in this study are described in Supplemental Tables 1 and 2.

**Animals and tumor models**

Mice were maintained according to guidelines of the Institutional Animal Care and Use Committee and irradiated using a RadSource RS-2000 X-Ray generator operating at 160 kv and 25 mA at a dose rate of 2.20 Gy/min, calibrated by NIST traceable dosimetry. To establish MCF7$^{GFP-IBD}$ tumors, 17β-estradiol pellets (1.7 mg, Innovative Research of America) were implanted in six-week-old athymic nude mice (Harlan Laboratories) 7 days before s.c. injection of $1 \times 10^7$ MCF7$^{GFP-IBD}$ cells in 100 µL of PBS.

8

Once tumors grew to 300 mm$^3$, 2 mg/mL doxycycline with 1% sucrose was added to the drinking water for 72 hours before irradiation. Mice were treated with pitavastatin (Atomole) by oral gavage (10 mg/kg or 30 mg/kg as indicated) 2 days before, the day of and 2 days after irradiation. Mice were treated with veliparib (ChemieTek) twice daily by oral gavage (25 mg/kg). IRIF formation in MCF7$^{GFP-IBD}$ tumors was analyzed at 3 and 24 hours after irradiation with 6 Gy. For B16.SIY tumors, C57BL/6 female mice (Harlan) were injected in the hind limb with 1 x 10$^6$ cells suspended in 100 µL PBS. After 8 to 12 days, mice were placed into treatment groups: control, 15 Gy, drug alone or drug + 15 Gy and treated with pitavastatin or veliparib as described above. Mice were maintained according to guidelines of the Institutional Animal Care and Use Committee.

**Clonogenic assays**

MCF7$^{GFP-IBD}$ and B16.SIY cells were plated at 100 cells per well in 6 well plates in triplicate in corresponding medium. 24 hours later, drugs were added 1 hour prior to irradiation. Radiation was delivered using a GammaCell $^{60}$Co source (MDS Nordion) with dose rate ranging from 10.5 to 9.4 cGy/sec depending on the date of the experiment. Cells remained in culture for 9-14 days and colonies of at least 50 cells were counted.

**Detection of DNA damage**

For neutral comet assays, cells were seeded at 1 x 10$^5$ per well in 6-well plates and treated as above. After 24 hours, cells were mixed with Comet LM agarose and single cell electrophoresis was performed on CometSlides (Trevigen). Slides were fixed, dried, stained with SYBR green (Thermo) and imaged on an Axiovert 40 with a 20X

9

Plan-NeoFluar objective and AxioCam camera. Two or more replicates were performed. Images were analyzed using an ImageJ comet assay macro (http://www.med.unc.edu/microscopy/resources/imagejplugins-and-macros/comet-assay).

For IRIF imaging, MCF7$^{\text{GFP-IBD}}$ cells were seeded on cover glass at 2.5 x 10$^4$ per well in 24 well plates. GFP-IBD expression was induced with 1 µg/mL doxycycline for 48 hours. Pitavastatin or other statins were added for 1 hour prior to IR. After 24 hours, cells were fixed, stained with 5 µg/mL Hoechst 33342, mounted using ProLong Gold (Invitrogen). Immunocytochemistry for γ-H2AX foci was performed using clone JBW301 (EMD Millipore). IRIF images were captured on an Axiovert 40CFL (Zeiss). Two or more replicates were performed.

**Histology and immunohistochemistry**

Formaldehyde-fixed paraffin-embedded (FFPE) tumor sections were stained with hematoxylin and eosin (H&E). Immunohistochemistry for Ki-67 was performed with clone SP6 (Lab Vision), ImmPRESS-AP (Vector Laboratories), Warp Red Chromogen Kit (Biocare Medical) and hematoxylin for counterstaining. H&E and Ki-67 imaging was conducted using an Axioskop upright microscope with a 10x/0.3NA objective, Axiocam digital color CCD camera and Zen imaging software (Zeiss). Immunofluorescence for γ-H2AX was performed using clone JBW301 (EMD Millipore) and imaged with an Axiovert 200M inverted fluorescence microscope with a 40x/1.3 NA objective (Zeiss), a CCD camera (Hamamatsu), and SlideBook imaging software (3i). ImageJ software (NIH) was used to prepare images for publication. A representative tumor sample from each group

10

was selected for analysis. Additional detail is provided in Supplementary Methods.

### SA-β-Gal assay

SA-β-Gal activity was determined on cell culture as well as frozen sections of excised tumors 7 days after IR. Cells were seeded at $3 \times 10^4$ per well in 6 well plates. Next day, cells were treated with drug for 1 hour prior to irradiation. Cells were fixed after 5 days and assayed for SA-β-Gal as described (35). SA-β-Gal positive and negative cells were counted in multiple fields, yielding an average percent SA-β-Gal positive staining, indicated on each SA-β-Gal image as mean ± SEM. Two or more replicates were performed. To evaluate senescence in vivo, 10-12 μm cryosections of OCT-embedded tumors were fixed in 2% paraformaldehyde, stained for SA-β-Gal activity, counterstained with nuclear fast red, dehydrated, mounted and imaged. A representative tumor sample from each group was selected for analysis.

### Statistical analysis

Statistical significance for IRIF counting and comet assays was determined using the non-parametric Mann-Whitney test. Calculations were performed using Prism software (GraphPad). *P* value ≤ 0.05 was considered statistically significant.

11

**RESULTS**

**Pitavastatin delays DNA repair and enhances senescence *in vitro* and *in vivo***

In prior work (18), we identified compounds that target DNA DSB repair by screening drug repurposing libraries against MCF7$^{GFP-IBD}$ human breast cancer cells irradiated with 6 Gy, using GFP-53BP1 as a live-cell imaging reporter for ionizing radiation-induced foci (IRIF) formation and resolution. Among diverse compounds found to promote IRIF persistence 24 hours after irradiation, we had identified two HMG-CoA reductase inhibitors in the NIH Clinical Collection library of agents with a history of use in Phase I, II or III clinical trials, the withdrawn agent cerivastatin (Baycol, Bayer) and the clinically used drug pitavastatin (Livalo, Kowa, Supplementary Fig. S1A, S1B and S1C). In secondary screens, pitavastatin significantly increased IRIF persistence at 24 hours as compared to cells treated only with radiation without increasing background IRIF over that of vehicle control ($P < 0.0001$, Fig. 1A and B).

Pitavastatin combined with ionizing radiation (IR) suppressed colony formation in irradiated MCF7$^{GFP-IBD}$ cells compared with IR alone, similar to the activity of the PARP1/2 inhibitor veliparib, a well established radiosensitizer (Fig. 1C). Radiosensitization of MCF7$^{GFP-IBD}$ cells by pitavastatin was dose-dependent (Supplementary Fig. S1D). While MCF7$^{GFP-IBD}$ cells displayed an $SF_2$ (surviving fraction at 2 Gy) of 0.54 for IR alone, addition of 1.25, 2.5 or 5 μmol/L pitavastatin reduced $SF_2$ to 0.4 ($P < 0.0001$), 0.29 ($P<0.001$) and 0.18 ($P < 0.0001$) respectively.

Pitavastatin also potentiated effects of radiation on cellular senescence *in vitro* (Fig. 1D). When combined with 6 Gy, 10 μmol/L pitavastatin increased the number of

12

large, flat cells expressing senescence-associated beta-galactosidase (SA-β-Gal) at 7 days after treatment to 84 ± 2% from 24 ± 3% with IR alone (P < 0.0001).

IRIF persistence and senescence induction were verified *in vivo* by treating mice bearing MCF7[GFP-IBD] tumor xenografts with pitavastatin and then irradiating the tumors with 6 Gy (Fig.1E, Supplementary Fig. S1E and S1F). Pitavastatin at 10 mg/kg markedly increased tissue destruction and SA-β-Gal activity after 6 Gy, a pattern similar to treatment with 10 mg/kg of the PARP inhibitor veliparib. While increasing pitavastatin to 20 mg/kg resulted in tumor tissue damage and increased SA-β-Gal activity on its own, the higher dose further potentiated the effects of radiation. While statins are taken continuously for lipid lowering, radiosensitization may require only transient treatment. Here, effects were observed with treatment limited to 2 days before, the day of irradiation and 2 days after.

To confirm that the effects of pitavastatin on IRIF persistence were mediated by inhibition of mevalonate biosynthesis, cells were treated with mevalonic acid, the metabolic intermediate produced by HMG-CoA reductase. 5 mM mevalonic acid was sufficient to restore IRIF resolution to MCF7[GFP-IBD] cells treated with pitavastatin (Fig. S2). In the absence of pitavastatin, while 5 mM mevalonic acid had no effect, 10 mM induced a small but significant acceleration of IRIF resolution.

Prior reports have ascribed greater anticancer activity to lipophilic statins (e.g. (36)), reflecting their greater effects on peripheral tissue versus the hepatoselectivity of hydrophilic statins. Thus, we compared the lipophilic statins pitavastatin, lovastatin, and simvastatin to the hydrophilic statins pravastatin, atorvastatin, and rosuvastatin for effects on DNA damage and DNA repair. None of the statins increased DNA damage on

13

their own at concentrations up to 10 µmol/L. Compared to DMSO control, the three lipophilic statins, pitavastatin, lovastatin and simvastatin, each induced IRIF persistence (from 11.1 ± 0.6 foci per nucleus to 16.6 ± 0.9, P< 0.0001, 17.1 ± 0.9, P < 0.0001, and 14.5 ± 0.8, P < 0.001, respectively) and increased % SA-β-Gal positive cells (from 21 ± 1.1 to 39 ± 5, P < 0.0001, 44 ± 1.5, P < 0.0001 and 45 ± 1.7, P< 0.0001). Hydrophilic statins pravastatin, atorvastatin and rosuvastatin each failed to potentiate IR with respect to IRIF persistence or senescence induction (Fig. 2A, B and C).

**Targeting the mevalonate pathway delays IRIF resolution and increases senescence in irradiated cells.**

To confirm the on-target activity of statins and identify the critical step(s) downstream of HMG-CoA reductase (HMGCR) which affect DNA repair, we applied shRNA to silence mevalonate pathway enzymes involved in cholesterol and isoprenoid intermediates biosynthesis (Fig. 3A). Stable MCF7$^{GFP-IBD}$ cell lines were obtained for two shRNAs for each target and scrambled control. Silencing of targeted protein was validated by Western blot (Supplementary Fig. S3). Much like treatment with pitavastatin, silencing HMGCR resulted in persistent DNA DSBs at 24 hours after IR as determined by neutral comet assay (Fig. 3B and C). These cells also displayed increased IRIF persistence and senescence induction (Fig. 3D and G). MCF7$^{GFP-IBD}$ cells expressing shRNA targeting, FDPS, the enzyme required for synthesis of FPP and GGPP and thus both types of prenylation displayed a similar phenotype to HMGCR silencing. The FDPS knockdown cells displayed elevated DNA damage, IRIF persistence and accelerated senescence after 6 Gy irradiation (Fig. 3B, C, D and G).

14

To distinguish which form of prenylation most impacts radiation sensitivity, we compared MCF7$^{GFP-IBD}$ cells expressing shRNAs silencing FNTB, farnesyl diphosphate transferase beta, or GGPS1, geranylgeranyl diphosphate synthase 1. To confirm inhibition of prenylation inhibition in pitavastatin treated or shRNA targeted cells we monitored the modification states of Hdj2 and Rap1, proteins known to be farnesylated and geranylgeranylated, respectively (37,38). Pitavastatin treatment or HMGCR silencing increased levels of unprenylated forms of both the Hdj2 and Rap1 proteins (Supplementary Methods and Supplementary Fig. S4). As expected, FNTB targeting increased unprenylated Hdj2 while GGPS1 silencing increased unprenylated Rap1.

Cells expressing shRNA targeted FNTB displayed delayed DSB repair, persistent IRIF and senescence induction after 6 Gy (Fig. 3E-G). Further implicating farnesylation as critical for DNA repair, farnesyl pyrophosphate restored DSB resolution in cells treated with pitavastatin (Supplementary Fig. S5). In contrast to FTNB, silencing GGPS1 to block protein geranylgeranylation failed to delay DSB repair. Effects on IRIF persistence were equivocal, but GGPS1 silencing increased SA-β-Gal positive senescent cells over scrambled control (Supplementary Fig. S6), suggesting distinct roles for farnesylated and geranylgeranylated proteins in DNA damage response.

**Pitavastatin enhances the growth delay after irradiation in B16.SIY mouse melanoma.**

To extend our results to a more physiological model, we examined radiosensitization by pitavastatin in the highly radioresistant B16.SIY transplantable murine melanoma cell line. Much like with the MCF7$^{GFP-IBD}$ human tumor cell line, we

15

observed a dose-dependent effect of pitavastatin on colony formation in B16.SIY cells (Fig. 4A and B). The SF2 value was 0.88 for IR alone and 0.7 when combined with 2.5 µmol/L pitavastatin ($P < 0.005$), yielding a dose modification factor (DMF) of 1.4, similar to that of the positive control veliparib (Supplementary Fig. S7). Clonogenic assays take into account different forms of cell death or proliferative arrest, including apoptosis, necrosis, mitotic catastrophe and senescence. To determine the contribution of cell death in pitavastatin-mediated radiosensitization, we performed cell viability assays at 48 hours after treatment. At 2.5 µmol/L, pitavastatin did not induce necrosis or apoptosis in B16.SIY cells nor increase cell death after irradiation (Supplementary Methods and Supplementary Fig. S8).

Pitavastatin significantly delayed DSB repair in B16.SIY cells after 6 Gy ($P < 0.0001$), with persistent damage reaching that of 12 Gy or 6 Gy plus 10 µmol/L veliparib (Fig. 4C and D). Similarly, pitavastatin enhanced B16.SIY senescence over radiation alone (Fig. 4E). Compared to $17 \pm 1\%$ SA-$\beta$-Gal positive cells formed by IR alone, combining 6 Gy with 1.0, 2.5 or 5.0 µmol/L pitavastatin yielded $66 \pm 2.3\%$, $P < 0.0001$, $67 \pm 2.2\%$, $P < 0.0001$, and $71 \pm 2\%$, $P < 0.0001$ respectively.

To examine radiosensitization *in vivo*, B16.SIY tumors were established and treated with pitavastatin, veliparib or a single dose of 15 Gy, or either drug in combination with IR. Pitavastatin and veliparib were applied 2 days before, the day of irradiation and the 2 days after. Tumors were excised at day 7 after the 15 Gy irradiation and analyzed by H&E for tissue integrity, IHC for $\gamma$-H2AX to detect persistent DNA damage, IHC for Ki-67 to assess cell proliferation, and SA-$\beta$-Gal to evaluate therapy-induced senescence. Imaging revealed treatment with either pitavastatin or veliparib

16

along with 15 Gy displayed increased tumor tissue destruction, increased DNA damage,

decreased cellular proliferation, and enhanced senescence (Fig. 5A). Neither

pitavastatin nor veliparib at a dose of 10 mg/kg appeared to affect tumor growth on their

own. Consistent with the low expression of the proliferation marker Ki-67 at day 7,

treatment with either pitavastatin or veliparib along with 15 Gy also conferred a

significant delay in tumor growth determined at day 12, compared to untreated, radiation

or either drug alone ($P < 0.01$, Fig. 5B and C).

17

## DISCUSSION

The first applications of ionizing radiation to cancer therapy began within months of Roentgen's report of X-ray imaging in 1895. While efforts to control and focus the delivered dose began early on, until recent decades, significant toxicities due to exposure of normal tissue could not be avoided. The prevailing strategy to limit normal tissue toxicity has been to "fractionate" radiotherapy by delivering small daily doses of 1.8 to 2.5 Gy/day. However, dramatic progress in computer-controlled radiation delivery has allowed tumors deep in the body to be treated with one or a few ablative doses of up to 25 Gy that produce dense DNA damage in the tumor while sparing surrounding normal tissue. Nonetheless, even with the most advanced tools, while tumor growth can often be delayed by radiation, local recurrence remains common. Further, high doses can only safely be delivered to small tumors. That precise delivery may not be sufficient on its own provides a rationale for developing radiosensitizers that can enhance genotoxic effects in the targeted field without increasing off-target toxicities. Given the positive relationship between radiation density and formation of DNA double strand breaks (DSBs), targeting repair of these potentially lethal lesions offers an attractive strategy.

Although molecularly targeted small-molecule DSB repair inhibitors have been pursued for several decades, progress to the clinic has been slow. A proven strategy to accelerate the path from discovery to clinical use is repurposing/repositioning of existing drugs (16,17,39,40). This may have particular value for discovery of radiosensitizers, based on identifying agents with well-established safety profiles that display previously unrecognized capacity to block DSB repair. To screen small molecules for effects on

18

DSB persistence, we have used a GFP fusion to the ionizing radiation-induced foci (IRIF) binding domain (IBD) of 53BP1 protein. GFP-IBD binds sites of H2AX phosphorylation to mark the chromatin domains that form around DSBs and then disperses upon DSB repair and H2AX dephosphorylation. Screening libraries of approved and investigational drugs, natural products, neutraceuticals and other small molecules identified numerous hits, including the HMG-CoA reductase inhibitors pitavastatin and cerivastatin (18).

Patients typically receive HMG-CoA reductase inhibitors to lower risks of cardiovascular disease. The cardiovascular benefits of statins are not ascribed solely to blocking cholesterol biosynthesis. Via inhibition of isoprenoid biosynthesis, statins also display pleiotropic effects mediated by decreased protein prenylation, primarily affecting small GTPases such as Rac and Rho (41). The prevalence of statin use among cancer patients has faciliated retrospective studies examining the potential impacts of HMG-CoA reductase inhibition on cancer incidence, progression and response to therapy. The convincing data for longer disease-free and/or overall survival after radiotherapy reported in prostate cancer (29,30) may reflect the role for dysregulated cholesterol metabolism in this disease (42,43) rather than a specific interaction with the DNA damage response. However, laboratory and clinical studies have reported radio- and/or chemo-sensitization in multiple cancers. Here, statin's effects may be linked to the DNA damage response, potentially decreased activity of small GTPases and other prenylated proteins such as lamins.

Our data support direct effects on DSB repair mediated by reduced prenylation. We observed persistent DNA damage, loss of clonogenic survival and increased

19

senescence when cells were treated with pitavastatin or other lipophilic statins along with radiation. Confirming an on-target effect, silencing the HMGCR HMG-CoA reductase or FDPS farnesyl diphosphate synthase recapitulated the effects of statins. In turn, the effects of pitavastatin could be suppressed by feeding cells mevalonic acid or farnesyl-pyrophosphate. Conversely, silencing the FNTB farnesyl transferase delayed DSB repair, while knock down of the GGPS1 geranylgeranyl phosphate synthase had no such effect. Taken together these observations suggest, that at least in part, decreased farnesylation of protein(s) may contribute to the effect of statin treatment on DNA repair. These data suggests new strategies and targets to develop radiosensitizers. A more complex pattern was observed with respect to the increased cellular senescence after radiation upon HMG-CoA reductase inhibition. Here, both FNTB and GGPS1 knockdown potentiated therapy-induced senescence after irradiation, suggesting roles for both farnesylated and geranylgeranylated proteins in this process.

To evaluate the impacts of HMG-CoA reductase inhibition on DNA damage response *in vivo*, we examined pitavastatin's effects on radiation response of tumors formed by the radioresistant melanoma cell line B16.SIY in syngeneic C57BL/6 mice. Pitavastatin had minimal effects on its own but strongly potentiated the effects of radiation. Combination therapy enhanced persistent DNA damage, decreased proliferation, increased senescence, and promoted tumor tissue destruction, leading to significant tumor growth delay compared to radiation alone.

Therapy-induced senescence has been proposed as a beneficial outcome of cancer therapy (3,4). Damaged cells that survive genotoxic stress may enter

20

senescence, thereby preventing a return to proliferation via undergoing terminal growth arrest (44,45). Senescence may also spread to nearby cells via a bystander effect (46). However, an offsetting concern is that senescent tumor cells may mediate adverse effects via paracrine signaling from the senescence associated secretory phenotype (SASP) that can promote inflammation and drive tumor cell proliferation, invasion, and metastasis (6,9,10). In prior work, we found that the PARP inhibitor veliparib delays DSB repair and promotes senescence after irradiation but modulates the SASP to decrease expression of inflammatory cytokines (12,35). Strikingly, our results both *in vitro* and *in vivo* demonstrated that non-toxic doses of pitavastatin display radiosensitizing properties that are at least equivalent to those of veliparib. Cardiovascular benefits of statins have long been ascribed to their anti-inflammatory properties along with their impact on lipid levels (47). Recently, it was shown that simvastatin can block senescent fibroblast secretion of SASP factors including inflammatory cytokines, an effect mediated by inhibition of protein prenylation (48). Thereby, simvastatin also suppressed the ability of the senescent cells to drive MCF7 breast cancer cell proliferation. The apparent similarities between effects of PARP inhibition and HMG-CoA reductase inhibition when combined with radiation are striking. Both block DSB repair and promote therapy-induced senescence but suppress secretion of inflammatory SASP factors. Nonetheless, given their distinct molecular targets and limited evidence of crosstalk between statins and PARP inhibitors, their common activities may not derive from a shared mechanism.

Taken together, our studies identify pitavastatin and other lipophilic statins as promising candidates for repurposing as nontoxic radiosensitizers. Our results are

consistent with retrospective studies in cancer patients (e.g. (29-32)) and provide a

mechanistic basis for these prior observations. Our data also suggest that the type of

statin and its dose may be critical, potentially explaining the wide range of effects

observed between patients and across studies. Supporting feasibility of translation to

the clinic, the pitavastatin dose required to demonstrate radiosensitization *in vitro* was

over 100 fold lower than peak plasma concentrations of pitavastatin reached by humans

taking standard doses. Interestingly, both lipophilic and hydrophilic statins have been

shown to decrease normal tissue damage after radiotherapy without protecting tumors

(e.g. (49-51)). Thus, together with prior studies, our results argue for repurposing HMG-

CoA reductase inhibitors such as pitavastatin or other lipophilic statins as agents to

enhance the therapeutic ratio of image-guided radiotherapy. Translation of these

observations via a clinical trial in a favorable situation such as treatment of prostate

cancer with curative intent appears justified.

22

23

## ACKNOWLEDGMENTS

23

## BIBLIOGRAPHY

1.    Moding EJ, Kastan MB, Kirsch DG. Strategies for optimizing the response of cancer and normal tissues to radiation. Nat Rev Drug Discov 2013;12(7):526-42.

2.    Ewald JA, Desotelle JA, Wilding G, Jarrard DF. Therapy-induced senescence in cancer. J Natl Cancer Inst 2010;102(20):1536-46.

3.    Nardella C, Clohessy JG, Alimonti A, Pandolfi PP. Pro-senescence therapy for cancer treatment. Nat Rev Cancer 2011;11(7):503-11.

4.    Acosta JC, Gil J. Senescence: a new weapon for cancer therapy. Trends Cell Biol 2012;22(4):211-9.

5.    Perez-Mancera PA, Young AR, Narita M. Inside and out: the activities of senescence in cancer. Nat Rev Cancer 2014;14(8):547-58.

6.    Davalos AR, Coppe JP, Campisi J, Desprez PY. Senescent cells as a source of inflammatory factors for tumor progression. Cancer Metastasis Rev 2010;29(2):273-83.

7.    Tchkonia T, Zhu Y, van Deursen J, Campisi J, Kirkland JL. Cellular senescence and the senescent secretory phenotype: therapeutic opportunities. J Clin Invest 2013;123(3):966-72.

8.    Velarde MC, Demaria M, Campisi J. Senescent cells and their secretory phenotype as targets for cancer therapy. Interdiscip Top Gerontol 2013;38:17-27.

24

9.      Pribluda A, Elyada E, Wiener Z, Hamza H, Goldstein RE, Biton M, et al. A senescence-inflammatory switch from cancer-inhibitory to cancer-promoting mechanism. Cancer Cell 2013;24(2):242-56.

10.     Demaria M, O'Leary MN, Chang J, Shao L, Liu S, Alimirah F, et al. Cellular Senescence Promotes Adverse Effects of Chemotherapy and Cancer Relapse. Cancer Discov 2016.

11.     Kang TW, Yevsa T, Woller N, Hoenicke L, Wuestefeld T, Dauch D, et al. Senescence surveillance of pre-malignant hepatocytes limits liver cancer development. Nature 2011;479(7374):547-51.

12.     Meng Y, Efimova EV, Hamzeh KW, Darga TE, Mauceri HJ, Fu YX, et al. Radiation-inducible immunotherapy for cancer: senescent tumor cells as a cancer vaccine. Mol Ther 2012;20(5):1046-55.

13.     Brown JS, O'Carrigan B, Jackson SP, Yap TA. Targeting DNA Repair in Cancer: Beyond PARP Inhibitors. Cancer Discov 2017;7(1):20-37.

14.     Samadder P, Aithal R, Belan O, Krejci L. Cancer TARGETases: DSB repair as a pharmacological target. Pharmacology & therapeutics 2016;161:111-31.

15.     Srivastava M, Raghavan SC. DNA double-strand break repair inhibitors as cancer therapeutics. Chemistry & biology 2015;22(1):17-29.

16.     Gupta SC, Sung B, Prasad S, Webb LJ, Aggarwal BB. Cancer drug discovery by repurposing: teaching new tricks to old dogs. Trends Pharmacol Sci 2013;34(9):508-17.

17. Bertolini F, Sukhatme VP, Bouche G. Drug repurposing in oncology--patient and health systems opportunities. Nature reviews Clinical oncology 2015;12(12):732-42.

18. Labay E, Efimova EV, Quarshie BK, Golden DW, Weichselbaum RR, Kron SJ. Ionizing radiation-induced foci persistence screen to discover enhancers of accelerated senescence. International journal of high throughput screening 2011;2:1.

19. Goglia AG, Delsite R, Luz AN, Shahbazian D, Salem AF, Sundaram RK, et al. Identification of novel radiosensitizers in a high-throughput, cell-based screen for DSB repair inhibitors. Molecular cancer therapeutics 2015;14(2):326-42.

20. Surovtseva YV, Jairam V, Salem AF, Sundaram RK, Bindra RS, Herzon SB. Characterization of Cardiac Glycoside Natural Products as Potent Inhibitors of DNA Double-Strand Break Repair by a Whole-Cell Double Immunofluorescence Assay. J Am Chem Soc 2016;138(11):3844-55.

21. Labay E, Mauceri HJ, Efimova EV, Flor AC, Sutton HG, Kron SJ, et al. Repurposing cephalosporin antibiotics as pro-senescent radiosensitizers. Oncotarget 2016;7(23):33919-33.

22. Aoki T, Nishimura H, Nakagawa S, Kojima J, Suzuki H, Tamaki T, et al. Pharmacological profile of a novel synthetic inhibitor of 3-hydroxy-3-methylglutaryl-coenzyme A reductase. Arzneimittel-Forschung 1997;47(8):904-9.

23. Winter-Vann AM, Casey PJ. Post-prenylation-processing enzymes as new targets in oncogenesis. Nat Rev Cancer 2005;5(5):405-12.

24. McTaggart SJ. Isoprenylated proteins. Cell Mol Life Sci 2006;63(3):255-67.

26

25.    Schonbeck U, Libby P. Inflammation, immunity, and HMG-CoA reductase inhibitors: statins as antiinflammatory agents? Circulation 2004;109(21 Suppl 1):II18-26.

26.    Sassano A, Platanias LC. Statins in tumor suppression. Cancer letters 2008;260(1):11-19.

27.    Sarrabayrouse G, Pich C, Teiti I, Tilkin-Mariame AF. Regulatory properties of statins and Rho GTPases prenylation inhibitiors to stimulate melanoma immunogenicity and promote anti-melanoma immune response. Int J Cancer 2017;140(4):747-55.

28.    Zhong S, Zhang X, Chen L, Ma T, Tang J, Zhao J. Statin use and mortality in cancer patients: Systematic review and meta-analysis of observational studies. Cancer Treat Rev 2015;41(6):554-67.

29.    Gutt R, Tonlaar N, Kunnavakkam R, Karrison T, Weichselbaum RR, Liauw SL. Statin use and risk of prostate cancer recurrence in men treated with radiation therapy. J Clin Oncol 2010;28(16):2653-9.

30.    Kollmeier MA, Katz MS, Mak K, Yamada Y, Feder DJ, Zhang Z, et al. Improved biochemical outcomes with statin use in patients with high-risk localized prostate cancer treated with radiotherapy. International journal of radiation oncology, biology, physics 2011;79(3):713-8.

31.    Mace AG, Gantt GA, Skacel M, Pai R, Hammel JP, Kalady MF. Statin therapy is associated with improved pathologic response to neoadjuvant chemoradiation in rectal cancer. Diseases of the colon and rectum 2013;56(11):1217-27.

32.  Lacerda L, Reddy JP, Liu D, Larson R, Li L, Masuda H, et al. Simvastatin radiosensitizes differentiated and stem-like breast cancer cell lines and is associated with improved local control in inflammatory breast cancer patients treated with postmastectomy radiation. Stem cells translational medicine 2014;3(7):849-56.

33.  Ostrau C, Hulsenbeck J, Herzog M, Schad A, Torzewski M, Lackner KJ, et al. Lovastatin attenuates ionizing radiation-induced normal tissue damage in vivo. Radiother Oncol 2009;92(3):492-9.

34.  Fritz G, Henninger C, Huelsenbeck J. Potential use of HMG-CoA reductase inhibitors (statins) as radioprotective agents. Br Med Bull 2011;97:17-26.

35.  Efimova EV, Mauceri HJ, Golden DW, Labay E, Bindokas VP, Darga TE, et al. Poly (ADP-ribose) polymerase inhibitor induces accelerated senescence in irradiated breast cancer cells and tumors. Cancer research 2010;70(15):6277-82.

36.  Campbell MJ, Esserman LJ, Zhou Y, Shoemaker M, Lobo M, Borman E, et al. Breast cancer growth prevention by statins. Cancer Res 2006;66(17):8707-14.

37.  Davis AR, Alevy YG, Chellaiah A, Quinn MT, Mohanakumar T. Characterization of HDJ-2, a human 40 kD heat shock protein. Int J Biochem Cell Biol 1998;30(11):1203-21.

38.  Adjei AA, Davis JN, Erlichman C, Svingen PA, Kaufmann SH. Comparison of potential markers of farnesyltransferase inhibition. Clin Cancer Res 2000;6(6):2318-25.

39.  Ashburn TT, Thor KB. Drug repositioning: identifying and developing new uses for existing drugs. Nat Rev Drug Discov 2004;3(8):673-83.

28

40.   O'Connor KA, Roth BL. Finding new tricks for old drugs: an efficient route for public-sector drug discovery. Nat Rev Drug Discov 2005;4(12):1005-14.

41.   Oesterle A, Laufs U, Liao JK. Pleiotropic Effects of Statins on the Cardiovascular System. Circulation research 2017;120(1):229-43.

42.   Wu X, Daniels G, Lee P, Monaco ME. Lipid metabolism in prostate cancer. American journal of clinical and experimental urology 2014;2(2):111-20.

43.   Yue S, Li J, Lee SY, Lee HJ, Shao T, Song B, et al. Cholesteryl ester accumulation induced by PTEN loss and PI3K/AKT activation underlies human prostate cancer aggressiveness. Cell metabolism 2014;19(3):393-406.

44.   Campisi J, d'Adda di Fagagna F. Cellular senescence: when bad things happen to good cells. Nat Rev Mol Cell Biol 2007;8(9):729-40.

45.   d'Adda di Fagagna F. Living on a break: cellular senescence as a DNA-damage response. Nat Rev Cancer 2008;8(7):512-22.

46.   Nelson G, Wordsworth J, Wang C, Jurk D, Lawless C, Martin-Ruiz C, et al. A senescent cell bystander effect: senescence-induced senescence. Aging Cell 2012;11(2):345-9.

47.   Jain MK, Ridker PM. Anti-inflammatory effects of statins: clinical evidence and basic mechanisms. Nat Rev Drug Discov 2005;4(12):977-87.

48.   Liu S, Uppal H, Demaria M, Desprez PY, Campisi J, Kapahi P. Simvastatin suppresses breast cancer cell proliferation induced by senescent cells. Sci Rep 2015;5:17895.

49.   Haydont V, Gilliot O, Rivera S, Bourgier C, Francois A, Aigueperse J, et al. Successful mitigation of delayed intestinal radiation injury using pravastatin is not

29

associated with acute injury improvement or tumor protection. International journal of radiation oncology, biology, physics 2007;68(5):1471-82.

50.    Mathew B, Huang Y, Jacobson JR, Berdyshev E, Gerhold LM, Wang T, et al. Simvastatin attenuates radiation-induced murine lung injury and dysregulated lung gene expression. American journal of respiratory cell and molecular biology 2011;44(3):415-22.

51.    Wedlake LJ, Silia F, Benton B, Lalji A, Thomas K, Dearnaley DP, et al. Evaluating the efficacy of statins and ACE-inhibitors in reducing gastrointestinal toxicity in patients receiving radiotherapy for pelvic malignancies. European journal of cancer (Oxford, England : 1990) 2012;48(14):2117-24.

**FIGURE LEGENDS**

**Figure 1.** Pitavastatin alters double strand break repair and promotes senescence in MCF7$^{GFP-IBD}$ cells and tumors. **A,** Pitavastatin blocks resolution of ionizing radiation induced foci (IRIF) in MCF7$^{GFP-IBD}$ cells. Cells were treated with 10 μmol/L pitavastatin or vehicle 1 hour prior to 6 Gy irradiation (IR). Representative images 24 hours after IR, showing IRIF reporter GFP-IBD (green), nuclear stain Hoechst 33342 (blue). Mean IRIF per nucleus ± SEM is indicated. Scale bar, 10 μm. **B,** IRIF per nucleus at 24 hours after IR in individual cells treated as in **A** are plotted. Red bar indicates mean ± SEM. ***, P < 0.001 (Mann-Whitney test). **C,** Clonogenic survival of MCF7 cells treated with 5 μmol/L pitavastatin or 10 μmol/L veliparib 1 hour prior to the indicated irradiation dose. Normalized survival fractions (■, IR alone; □ IR + pitavastatin; ○ IR + veliparib) for representative data are shown. Each data point represents an average of 3 replicates. **D,** Senescence induction was evaluated in MCF7$^{GFP-IBD}$ cells treated with pitavastatin or vehicle 1 hour prior to 6 Gy by SA-β-Gal (blue) staining 5 days post IR. Mean percent SA-β-Gal$^+$ cells ± SEM indicated. Scale bar 50 μm. **E,** Mice bearing MCF7$^{GFP-IBD}$ tumor xenografts were treated with pitavastatin 2 days before, the day of, and for 2 days after 6 Gy irradiation. Tumors were harvested 5 days after IR, sectioned and stained for SA-β-Gal activity (blue). Representative images from different treatment groups are shown. Scale bar 50 μm.

**Figure 2.** Lipophilic statins enhance IRIF persistence and senescence in irradiated MCF7$^{GFP-IBD}$ cells *in vitro.* **A,** Cells were treated with 10 μmol/L of lipophilic statins pitavastatin, lovastatin, or simvastatin, or the hydrophilic statins pravastatin, atorvastatin

31

or rosuvastatin, or vehicle 1 hour prior to IR with 6 Gy. Representative images of GFP-IBD localization (green) and Hoechst 33342 staining (blue) in non-irradiated cells and cells 24 hours post IR are shown. IRIF per nucleus is indicated as mean ± SEM. Scale bar, 10 µm. **B,** Plot of IRIF per nucleus in individual cells treated as indicated. Red bar indicates mean ± SEM. ***, P < 0.0001; **, P < 0.001; ns – non significant (Mann-Whitney test). **C,** MCF7$^{GFP-IBD}$ cells were treated as in **A** and senescence evaluated by SA-β-Gal staining (blue) 5 days post treatment. Percent SA-β-Gal positive cells is indicated as mean ± SEM. Scale bar 50 µm.

**Figure 3.** Targeting the mevalonate pathway via silencing of HMGCR, FDPS or FNTB delays DSB repair, prolongs IRIF persistence and promotes senescence after irradiation of MCF7 cells. **A,** Mevalonate pathway with targeted enzymes in red. **B,** Cell lines stably expressing shRNA targeting HMGCR, FDPS, or scrambled control were irradiated with 6 Gy. Representative images from neutral comet assay 24 hours post IR are shown. Percent tail DNA ± SEM shown. **C,** Plot of percent tail DNA. Red line indicates mean ± SEM. ***, P < 0.0001; **, P < 0.001; ns – non significant (Mann-Whitney test). **D,** IRIF persistence in irradiated MCF7 cells after knockdown of HMGCR or FDPS shown by γ-H2AX foci (yellow) and Hoechst 33342 staining (blue) in representative cells 24 hours after IR. Two shRNA constructs confer similar effects for each target. Scale bar 10 µm. **E,** Plot of comet percent tail DNA in FNTB knockdowns. Red line indicates mean ± SEM. ***, P < 0.0001, (Mann-Whitney test). **F,** IRIF persistence after knockdown of FNTB shown by γ-H2AX (yellow) and Hoechst 33342 (blue) after 24 hours. Scale bar 10 µm. **G,** Senescence induction in cells bearing shRNA targeting HMGCR, FDPS or FNTB

evaluated by SA-β-Gal (blue) 5 days after 6 Gy. Representative images from three experiments are shown. Percent SA-β-Gal positive cells is indicated as mean ± SEM. Scale bar 50 μm.

**Figure 4.** Pitavastatin radiosensitizes B16.SIY murine melanoma *in vitro*. **A,** Clonogenic survival of B16.SIY cells treated with indicated concentration of pitavastatin. Representative images shown with mean colonies ± SEM from three replicates. **B.** Clonogenic survival of B16.SIY cells treated with 2.5 μmol/L pitavastatin 1 hour prior to the indicated irradiation dose. Normalized survival fractions (■, IR alone; ○, IR + pitavastatin) indicating the average of 3 replicates. **C,** Neutral comet assay of B16.SIY cells treated with 25 μmol/L veliparib (positive control) or 10 μmol/L pitavastatin for 1 hour prior to IR. Representative images with percent tail DNA ± SEM. **D,** Percent tail DNA, with mean ± SEM. ** P <0.001; ***, P < 0.0001, Mann-Whitney test. **E,** Senescence induction evaluated by SA-β-Gal (blue) staining of B16.SIY cells 5 days after treatment with 1 μmol/L, 2.5 μmol/L and 5 μmol/L pitavastatin or 25 μmol/L veliparib 1 hour prior to 6 Gy. Percent SA-β-Gal^{+} cells indicated as mean ± SEM. Scale bar 50 μm.

**Figure 5.** Pitavastatin radiosensitizes B16.SIY murine melanoma *in vivo*. **A,** Mice bearing B16.SIY tumors were treated with 10 mg/kg pitavastatin or veliparib daily by gavage two days before, the day of, and two days after a single dose of 15 Gy. After 7 days, tumors were excised and examined by hematoxylin and eosin (H&E), γ-H2AX IHC, Ki-67 IHC and SA-β-Gal. Note marked tissue destruction, high residual DNA damage,

33

low proliferation and high senescence in tumor treated with pitavastatin + IR.

Representative images are shown. Scale bar 100 µm. **B,** B16.SIY tumor growth was

tracked in mice treated with pitavastatin or veliparib and/or 15 Gy as in **A**. N=7 per

group for control, 15 Gy, pitavastatin, veliparib, pitavastatin + 15 Gy, veliparib + 15 Gy.

Mean ± SD shown. **C,** Scatter plot of individual tumor volumes from **B** at day 12, with
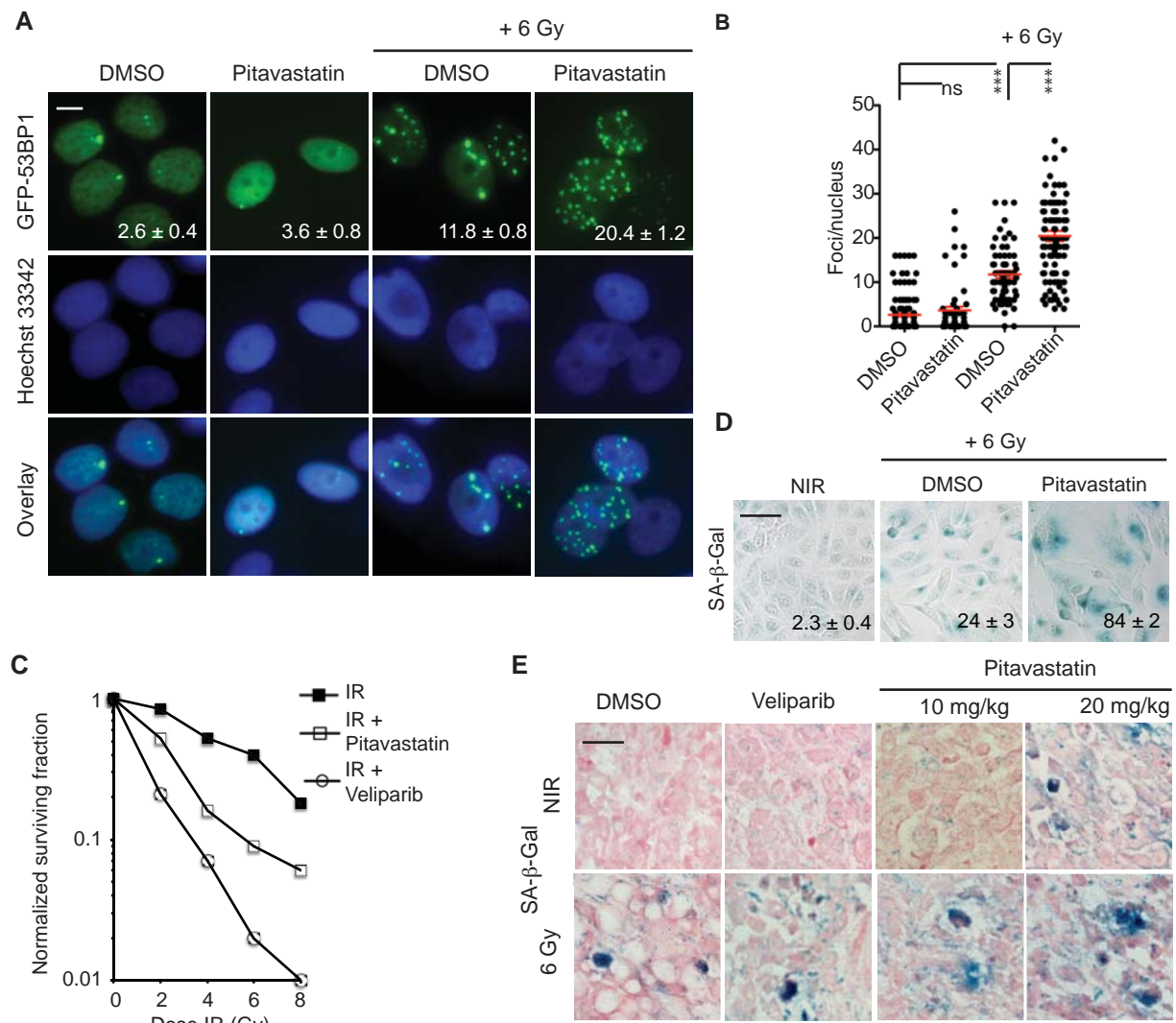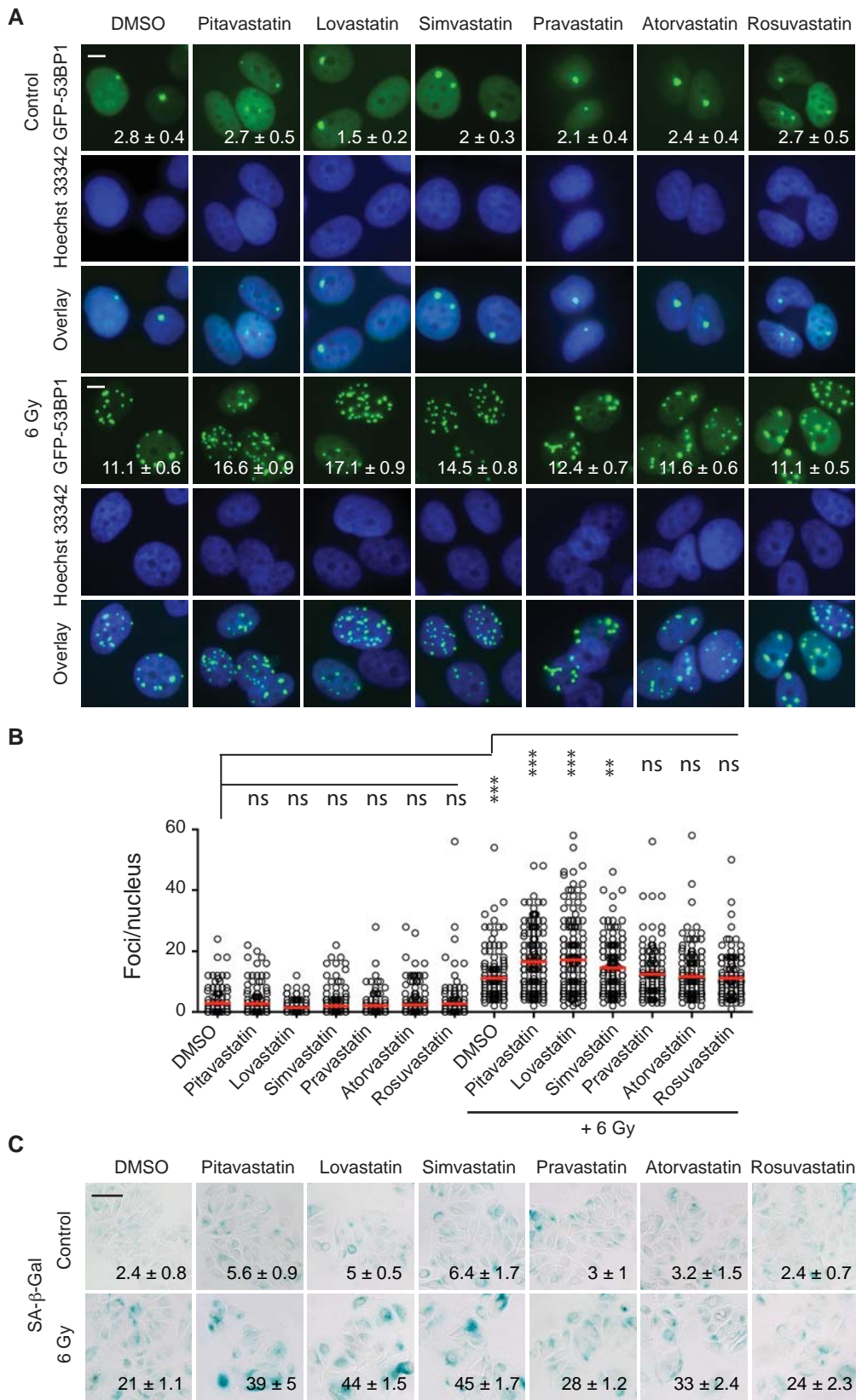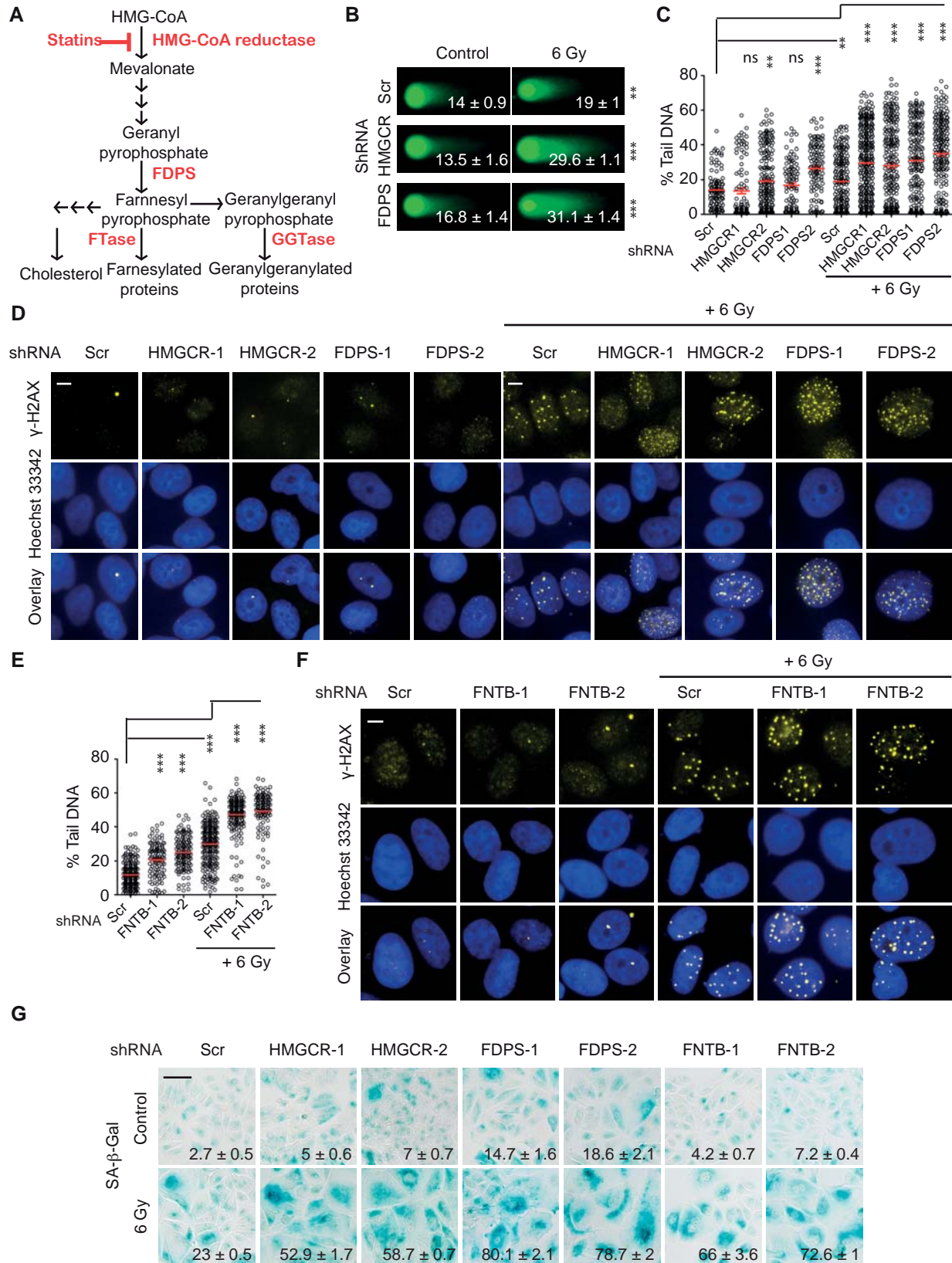
mean ± SEM.

Figure 1

Figure 2

Figure 3

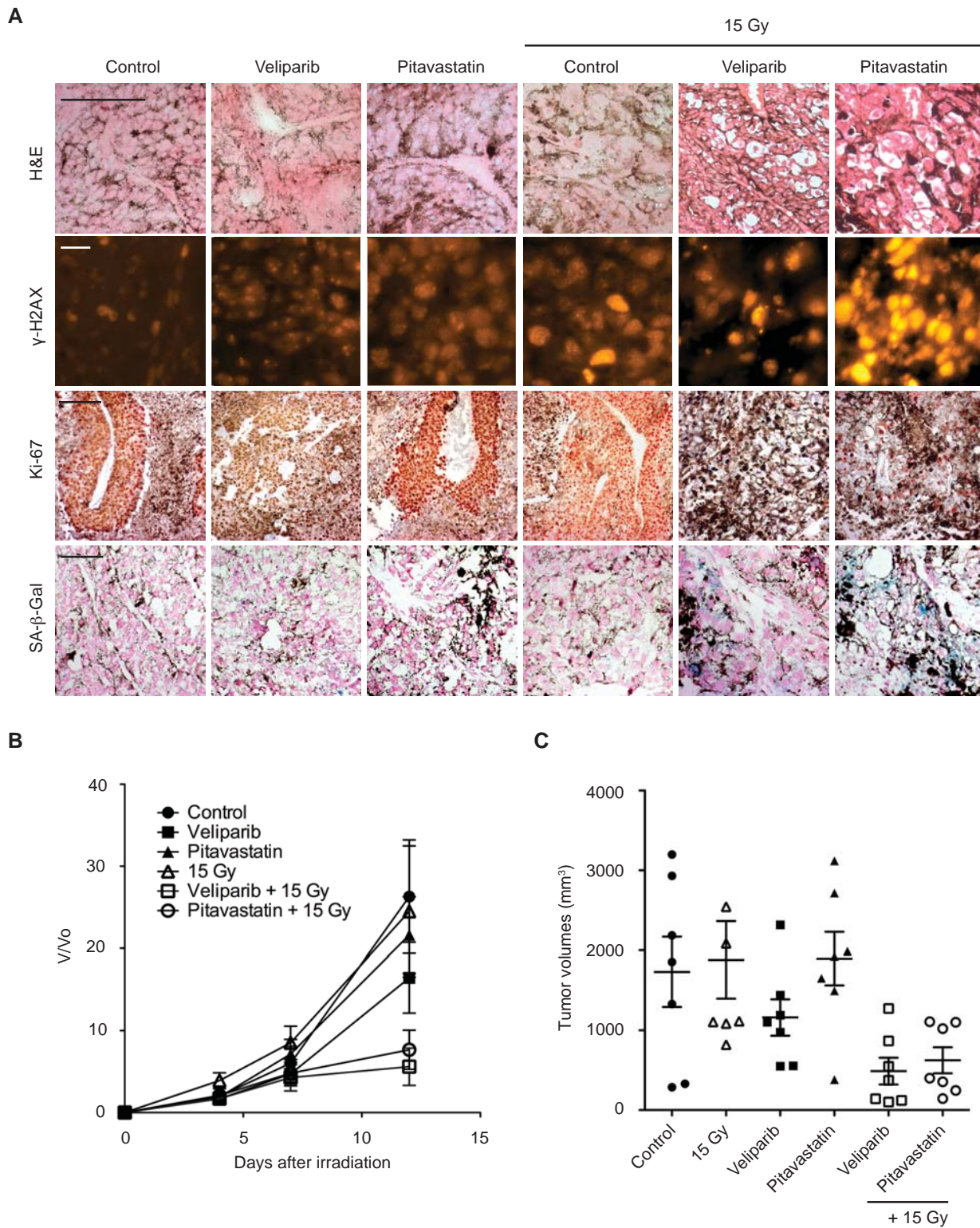Figure 4

Figure 5

AACR  American Association
for Cancer Research
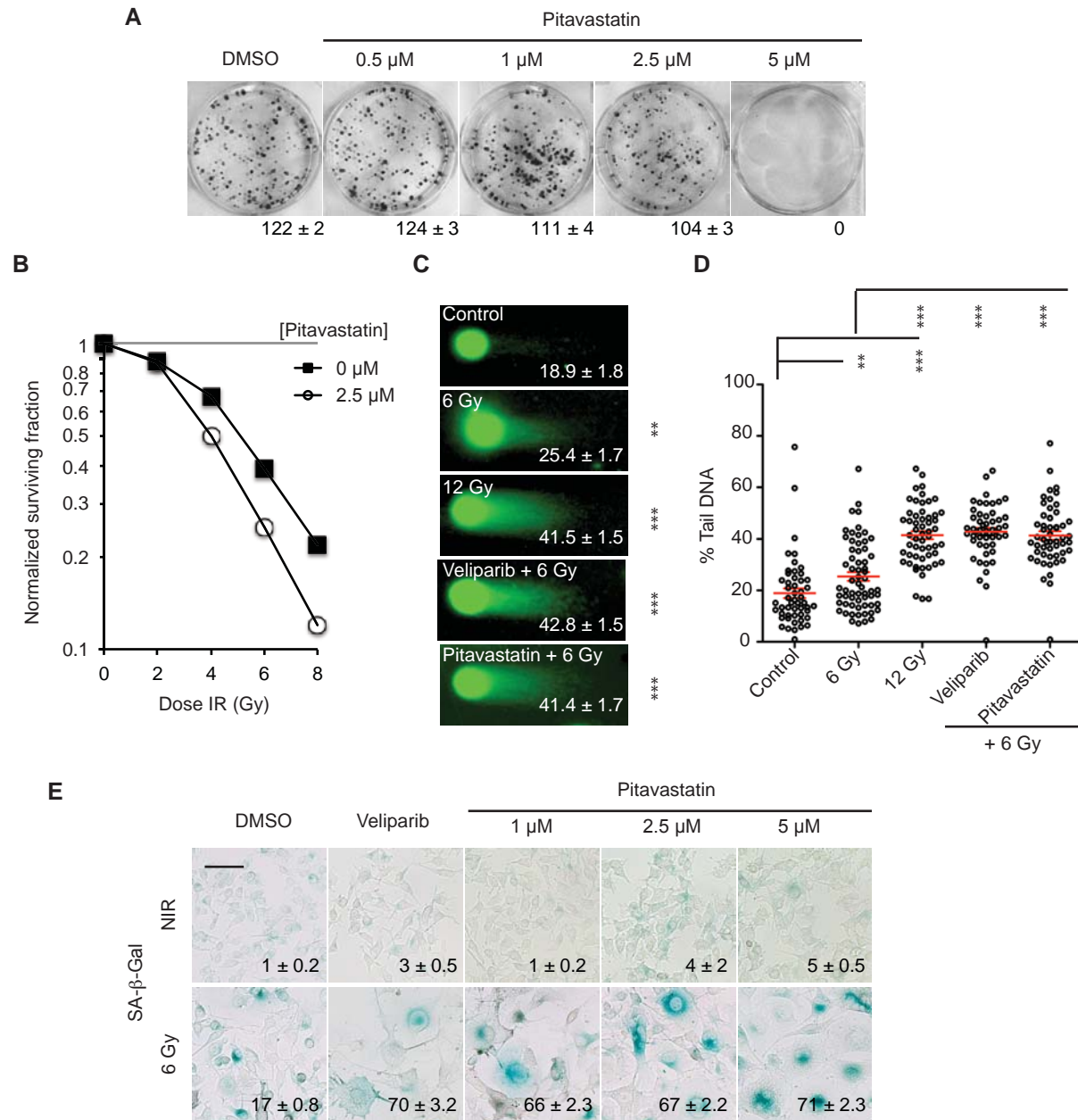
# Molecular Cancer Therapeutics

# HMG-CoA reductase inhibition delays DNA repair and promotes senescence after tumor irradiation

Elena V. Efimova, Natalia Ricco, Edwardine Labay, et al.

| | |
|---|---|
| **Updated version** | Access the most recent version of this article at:<br>doi:10.1158/1535-7163.MCT-17-0288 |
| **Supplementary Material** | Access the most recent supplemental material at:<br>http://mct.aacrjournals.org/content/suppl/2017/09/22/1535-7163.MCT-17-0288.DC1 |
| **Author Manuscript** | Author manuscripts have been peer reviewed and accepted for publication but have not yet been edited. |

| | |
|---|---|
| **E-mail alerts** | Sign up to receive free email-alerts related to this article or journal. |
| **Reprints and Subscriptions** | To order reprints of this article or to subscribe to the journal, contact the AACR Publications Department at pubs@aacr.org. |
| **Permissions** | To request permission to re-use all or part of this article, use this link<br>http://mct.aacrjournals.org/content/early/2017/10/13/1535-7163.MCT-17-0288.<br>Click on "Request Permissions" which will take you to the Copyright Clearance Center's (CCC)<br>Rightslink site. |